JOURNAL OF MATERIALS SCIENCE **34** (1999) 4293–4304

Morphology of and surface modification by TiO_2 deposits on a porous ceramic substrate

SHU-CHUAN HUANG, TONG-FONG LIN, SHIH-YUAN LU *, KAN-SEN CHOU
Department of Chemical Engineering, National Tsing-Hua University, Hsin-Chu, Taiwan 30043, Republic of China 886-3-571-4364
E-mail: sylu@che.nthu.edu.tw

We investigate the morphology of and surface modification by titanium dioxide (TiO_2) deposits on porous ceramic substrates placed in a horizontal, tubular, hot-wall, atmospheric pressure chemical vapor deposition (CVD) reactor with titanium tetraisoperoxide (TTIP) as the precursor. The TiO_2 particles are produced from TTIP through two routes: first by thermal decomposition which then kicks off hydrolysis. The deposit characteristics is found to be location dependent. Those at the reactor entrance and exit are different from that within the reactor. Within the reactor, the deposit characteristics is further found to depend strongly on the deposition temperature (T_d) and is almost independent of the flow-rate and concentration of the reactant. With a T_d of about 380 °C, the deposited TiO_2 forms a forest-like structure with poor adhesivity to the substrate and results in an insignificant pore size reduction for the substrate. If T_d drops down to about 300 °C, the deposited TiO_2 forms a rock-packing structure with good adhesivity to the substrate and can reduce the pore size of the substrate from about 1–2 μm down to about 64 nm. At both the reactor entrance and exit, the deposited TiO_2 are loosely-packed spherical particles of average diameter of 140–400 nm. A theory, based on whether or not the reaction is gas-phase or surface dominated, is proposed to explain the dramatic effect of T_d.

1. Introduction

Titanium dioxide, because of its many advantageous properties such as high dielectric constant, excellent optical transmittance, high refractive index, high chemical stability, and a suitable band gap, has found extensive applications in industrial products such as capacitors, optical coatings, sensors, catalyst supports, and photocatalysts [1]. Its use as a photocatalyst is of particular interest to the waste water treatment research community since it can decompose many hazardous organic substances into disposable ones [2, 3] while retaining its own chemical integrity.

One efficient way of utilizing the photocatalytic ability of TiO_2 is to incorporate fine TiO_2 particles as a top layer of a membrane reactor. A membrane reactor is a reactor capable of removing products from reactants via membrane separation thus enhancing the forward reaction. A ceramic membrane normally consists of a porous support covered with one or more ceramic layers with decreasing pore sizes. The reduction in and control of pore size is of essential importance to the separation performance of the ceramic membrane. Depending on application requirements, the pore size of the top layer of the membrane can range from about one micron meter for micro-filtration to less than one nanometer for gas separations. As a top layer of a membrane reactor, the TiO_2 deposit serves as both the catalyst and separation medium.

Basically, there are two routes to deposit particles onto the porous support. One is wet chemistry based such as the sol-gel method, and the other is gas phase based such as the chemical vapor deposition process. The chemical vapor deposition process has been gaining popularity in recent years since it is a cleaner, more energy-effective, environmentally sounder way of depositing fine particles than the more traditional wet chemistry methods [4, 5]. The effectiveness of this method in forming a top layer for ceramic membranes depends on how effective it is in reducing the pore size of the support and whether or not this top layer is firmly incorporated onto the support.

Tsapatsis and Gavalas [6] performed CVD of SiO_2 and other oxides on porous Vycor tubes for preparing hydrogen separation membranes capable of being operated at elevated temperatures. Xomeritakis and Lin [7] have also carried out the research on forming thin inorganic oxide layers via CVD processes. Yan and coworkers [8] coated the outer surface of an α-alumina porous tube with boehmite sol, which was calcined into a γ-alumina layer of pore size around 7 nm. These pores were then filled with SiO_2 formed by thermally activated CVD of tetraethyl orthosilicate in 400–600 °C.

* Author to whom all correspondence should be addressed.

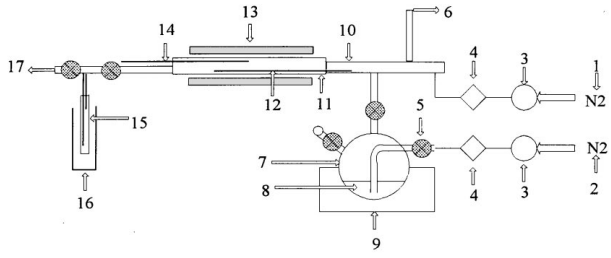

1. dilution gas
2. carrier gas
3. moisture trap
4. mass flow controller
5. valve
6. vacuum gauge
7. bubbler
8. precursor
9. isothermal bath
10. pre-furnace zone
11. quartz tube
12. substrate transferring rod
13. furnace
14. thermal couple
15. cold trap
16. ice bath
17. pump

Figure 1 Schematic diagram of CVD system used for deposition of TiO_2 particles.

In this work, we studied the morphology of TiO_2 particles as deposited on top of a porous ceramic support through the CVD process by using TTIP as the precursor. And then the effectiveness of the deposited TiO_2 layer in pore size reduction is evaluated by the N_2 permeation experiments. The relation between the surface modification capability and the deposition condition of the TiO_2 deposit is investigated.

2. Experimental

2.1. Chemicals

Argon (99.995%), helium (99.995%), and nitrogen (99.995%) are all purchased from LH Gas Company in Taiwan. Acetone (99.5%) and sulfuric acid (97.3%)

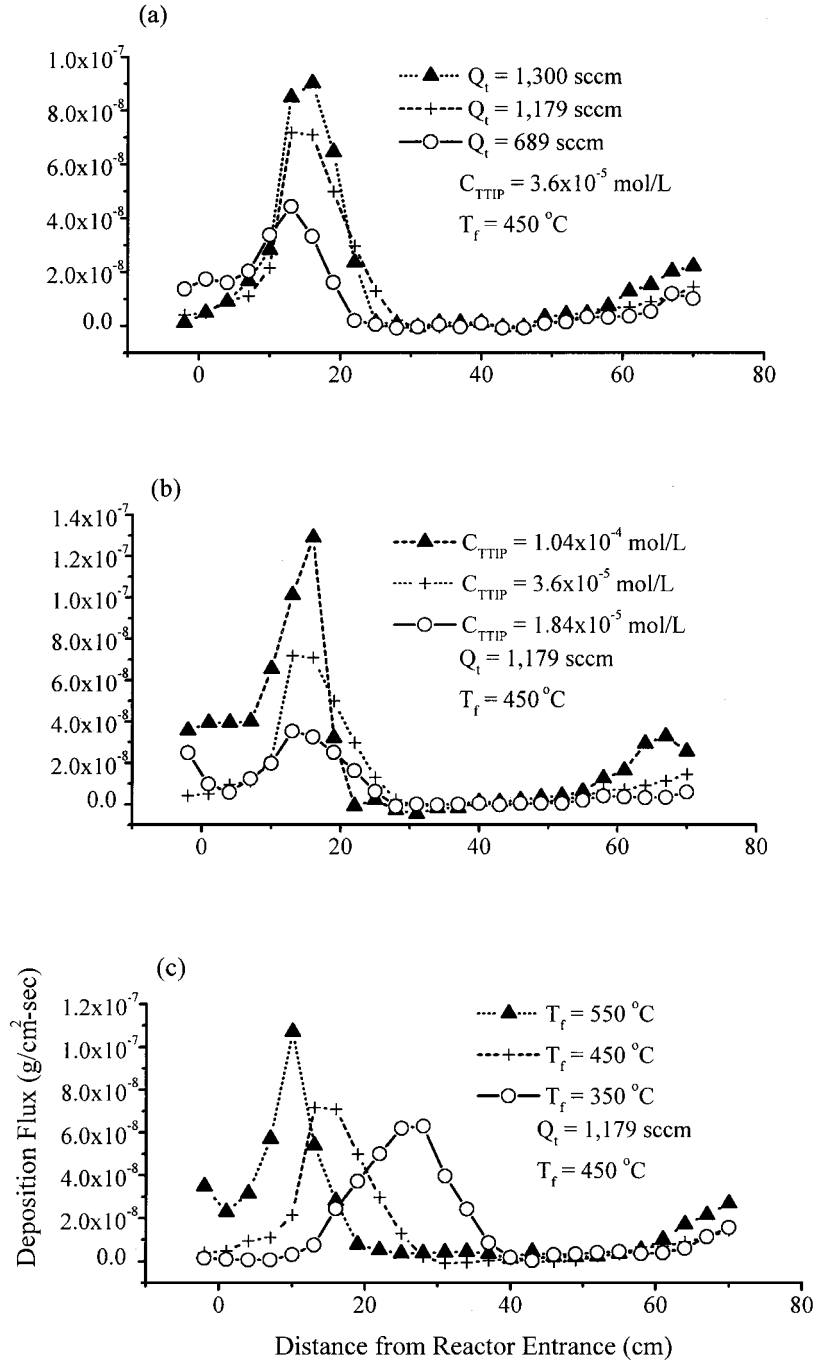

Figure 2 The effect of (a) Q_t, (b) C_{TTIP}, and (c) T_f on the deposition flux of TiO_2 particles.

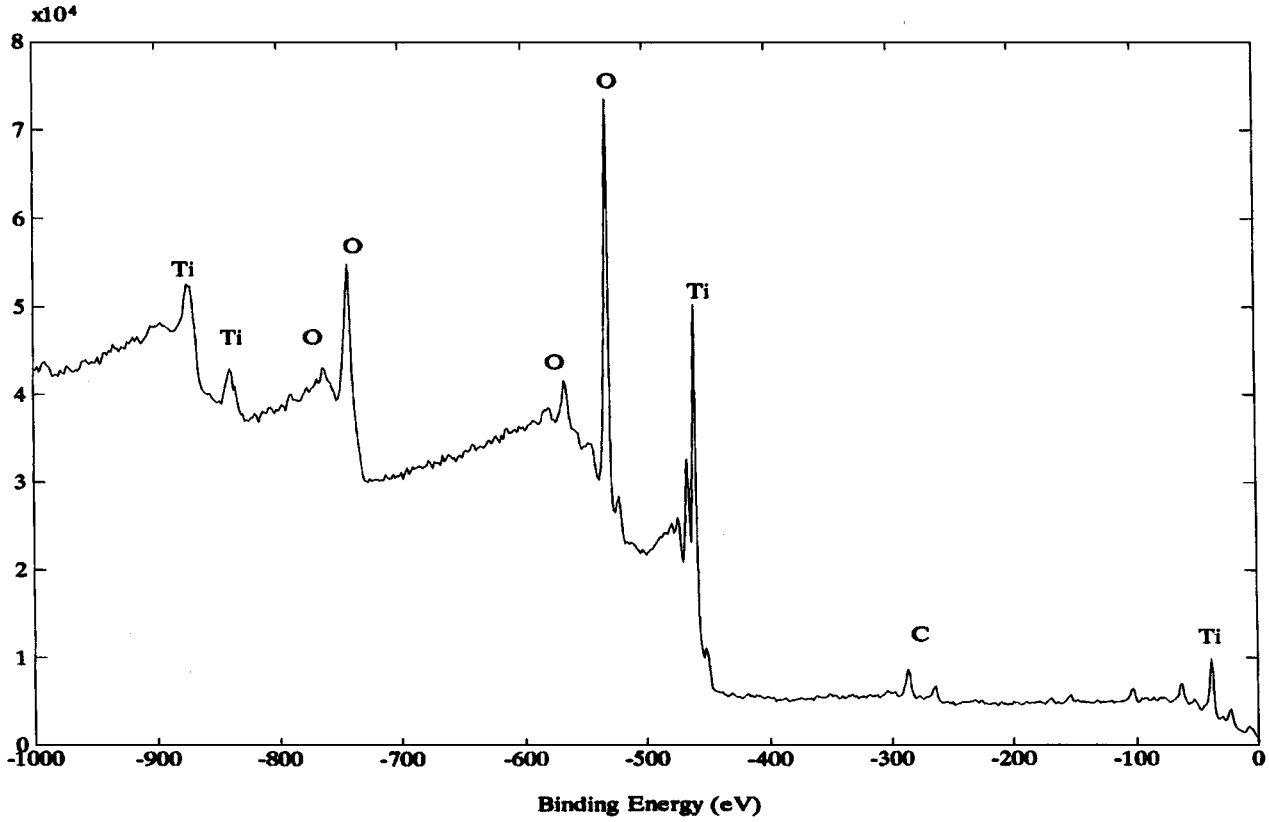

Figure 3 The ESCA plot of TiO_2 as deposited on a silicone substrate.

are both from Union Chemical Works while titanium tetraisoproxide is from Janssen.

2.2. Deposition processes

Fig. 1 shows the schematic diagram for the CVD setup used in this study. It is a horizontal, tubular, hot-wall, atmospheric pressure chemical vapor deposition system. Nitrogen gas is used as both the dilution gas and the carrier gas. Flow rates of gases are controlled by Precision 401 Mass Flow Controllers. A bubbler is used to hold the water-sensitive precursor. Transferring of the moisture-sensitive precursor, TTIP, is carried out in a drybox to prevent TTIP from hydrolysis. A Polyscience isothermal bath is used to control the evaporating temperature of the precursor. A BriskHeat heating tape with an ANC-607 temperature controller is used to heat the zone before the furnace to avoid the condensation of TTIP vapor before flowing into the reactor. The heating tape is set at a temperature 10 °C above that of the isothermal bath. The reaction chamber is a quartz tube with an O.D. of 40.69 mm, an I.D. of 36.64 mm, and a length of 97.5 cm. A 67 cm long Lenton furnace with an Eurotherm temperature controller provides controlled heating for the reaction chamber.

Substrates, including quartz rings and homemade porous ceramic disks, are cleaned with deionized water and dried at 100 °C for at least 8 h. The porous ceramic disks are fabricated by mixing appropriate amount of carboxyl methylcellulose (CMC), water, kaolin and α-alumina, followed by the processes of drying, milling, meshing, pressing at 4000 pounds, and firing. A detailed fabrication procedure can be found in Chou *et al.* [9]. The porous ceramic disks are white in color and have an O.D. of 38 mm, a thickness of 1.6 mm, and an average pore size of approximately 1–2 μm. Quartz rings are used for determination of the deposition flux of TiO_2 particles at the wall. When quartz rings are reused, they are soaked in hot (120 °C) concentrated sulfuric acid for several hours to remove residual TiO_2 particles. They are then washed with deionized water, sonicated, and dried before they are weighed and placed in the quartz tube reactor.

The bubbler which contains the precursor is placed in an isothermal bath set at a desired temperature. The whole CVD reactor is then evacuated to a pressure of about 10^{-2} torr. The furnace is then heated to a desired temperature for at least one hour while the evacuation continues. The dilution gas is then introduced into the reactor to purge the CVD system for 30 min. After the

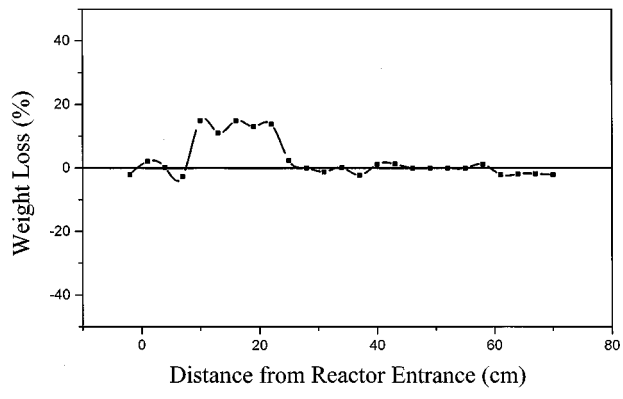

Figure 4 The weight loss percentage distribution along the reactor length.

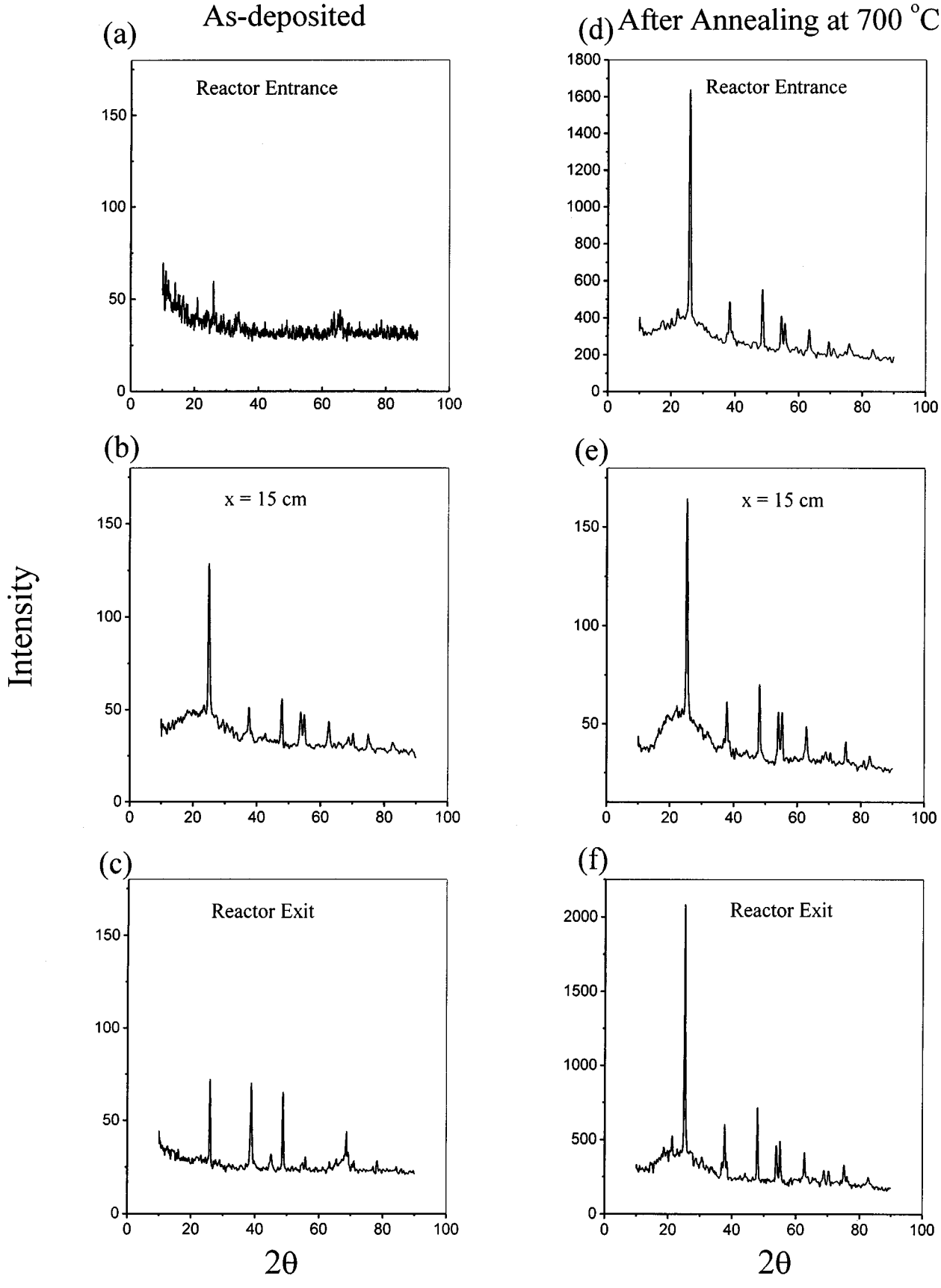

Figure 5 The powder XRD of TiO_2 particles under the base condition as deposited on the quartz rings at (a) the reactor entrance, (b) $x = 15$ cm, and (c) the reactor exit before annealing, and after annealing at (d) the reactor entrance, (e) $x = 15$ cm, and (f) the reactor exit.

pressure of the system reaches about 10^{-2} torr, the TTIP containing bubbler is then immersed in the isothermal bath. Titanium tetraisoproxide [Ti-(O-*i*-$C_3H_7)_4$] is a colorless liquid with a boiling point of 232 °C and a density of 0.955 g/cm^3. Its vapor pressure can be found from the catalog of Tri-Chemicals.

The region between the bubbler and the entrance of the furnace is wrapped with a heating tape and the

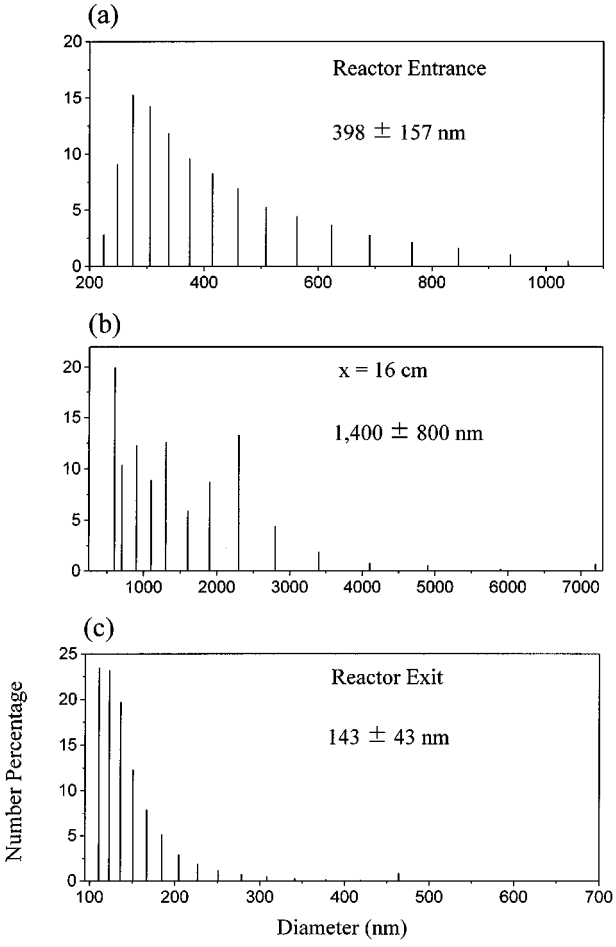

Figure 6 Size distributions of TiO_2 particles collected at (a) the reactor entrance, (b) $x = 16$ cm, and (c) the reactor exit under the base condition.

temperature of the heating tape is set at a temperature 10 °C higher than that of the isothermal bath. After the temperature has become stable, the pump was turned off and the dilution gas (N_2) was brought into the system to raise the pressure of the system back to one atm. Finally, the carrier gas is introduced to carry the precursor into the reactor for the deposition of TiO_2 particles.

For the present study, the furnace temperature (T_f) varies from 350 to 550 °C, the temperature of the isothermal bath (T_b) from 70 to 105 °C, the flow rate of the dilution gas (Q_d) from 510 to 1000 sccm, and the flow rate of the carrier gas (Q_c) from 179 to 300 sccm. To ease the parametric study, we select a base condition around which the relevant operating conditions are varied. At this base condition, T_f is set at 450 °C, T_b at 85 °C, Q_d at 1000 sccm, and Q_c at 179 sccm. Under this condition, the inlet concentration of TTIP based on 25 °C (C_{TTIP}) is 3.6×10^{-5} mol/l and the total flow rate of gases (Q_t) is 1,179 sccm. This condition will be later referred to as the "base condition."

2.3. Characterizations

Deposition fluxes, morphology, crystalline phases, particle sizes, compositions and pore sizes of TiO_2 deposits are determined. Scanning electron microscopy (SEM) is performed with the Jeol SEM 804A to observe the morphology, the particle size and the thickness of the deposited TiO_2 layer. The Shimadzu XD-5 X-ray diffractometer with CuK_α (1.5405 Å) is used to determine the crystalline phase of the particles. The Otsuka Electronics LPA-300 particle size analyzer is used to determine the size distribution of TiO_2 particles. The Physical Electronics PHI 1600 Electron Spectroscopy for Chemical Analysis (ESCA) is used to determine the composition of the deposit. The pore size of the porous ceramics with or without TiO_2 deposits can be determined by the gas permeation experiments [10].

3. Results and discussion

3.1. Deposition fluxes

The effect of T_f, C_{TTIP}, and Q_t on the deposition flux is studied. For referring convenience, when Q_t, C_{TTIP} or T_f is not specified, it is set at the base condition value. Quartz rings are placed in the quartz tube for measuring TiO_2 deposition fluxes along the axis of the reactor. These quartz rings are of an I.D. of 31.25 mm and a length of 20 mm. Deposition fluxes are determined by the weight pickup resulting from the reaction, quartz ring inner area, and total reaction time. Typically, the deposition flux increases with increasing axial position (x), reaches a maximum, drops down to almost zero, and finally goes up again near the reactor exit. This trend is the same with that observed by Kirkbir and Komiyama [11] on the production of TiO_2 particles from TTIP. A modeling work by Lu and Lin [12] for the oxidation of $TiCl_4$ in a tubular CVD reactor also shows the same trend in deposition flux.

Basically, the reaction of TTIP to form TiO_2 becomes more intense when the reactants flow into the reactor and are heated to a higher temperature. This results in higher production rate of TiO_2 and thus higher deposition rate of TiO_2. After reaching a maximum, the deposition flux must decrease since the concentration of TiO_2 in the main stream has been dropping. The concentration of TiO_2 eventually drops to a level that the driving force for diffusional deposition is no longer strong enough to move particles towards the wall. This situation persists until near the reactor exit where, due to the cooling effect of the non-heated outside surrounding, the remaining main stream particles are again pushed towards the wall by the thermopheretic force caused by the temperature gradient across the tube.

The effect of C_{TTIP} and Q_t on deposition fluxes is shown in Figs 2a and b, respectively. The higher the Q_t or C_{TTIP}, the larger the deposition flux. This is no surprise since increasing of either Q_t or C_{TTIP} increases the amount of TTIP available to form TiO_2 particles. Increase in Q_t or C_{TTIP} however does not appreciably shift the peak of the deposition flux since the reaction and thus deposition are more dominated by the system temperature. Interestingly, for the case of Q_t at 689 sccm, deposition fluxes between x of 0–10 cm are higher than those for higher Q_ts. This may be due to the prolonged residence time, that gives more time for reaction and deposition, for this low Q_t.

The effect of T_f on deposition fluxes is shown in Fig. 2c. Deposition fluxes of TiO_2 reach a maximum at approximately $x = 29$, 13, and 10 cm for T_f of 350,

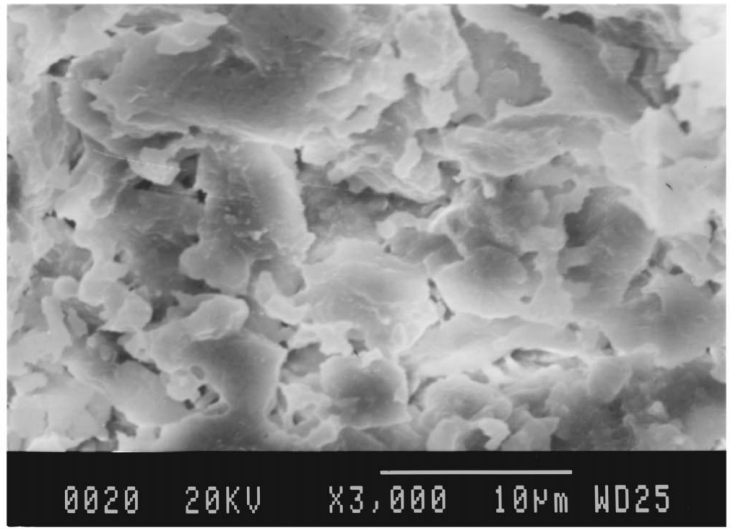

(a)

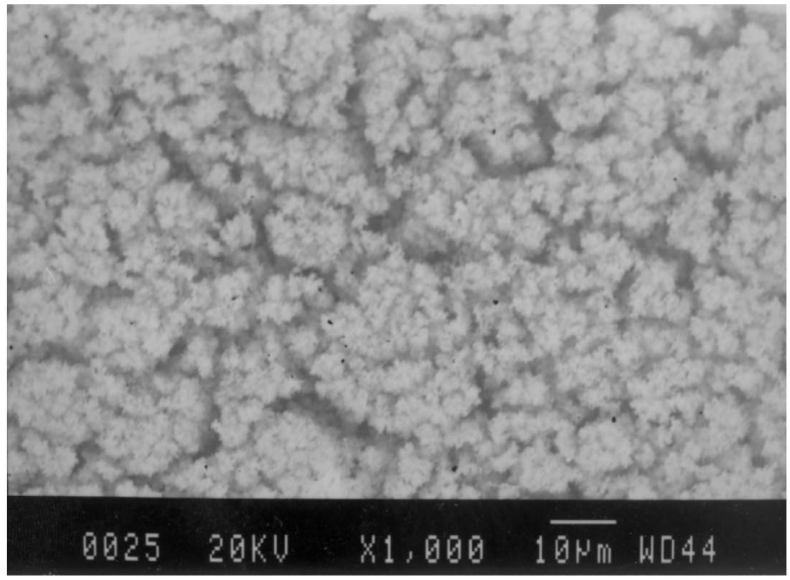

(b)

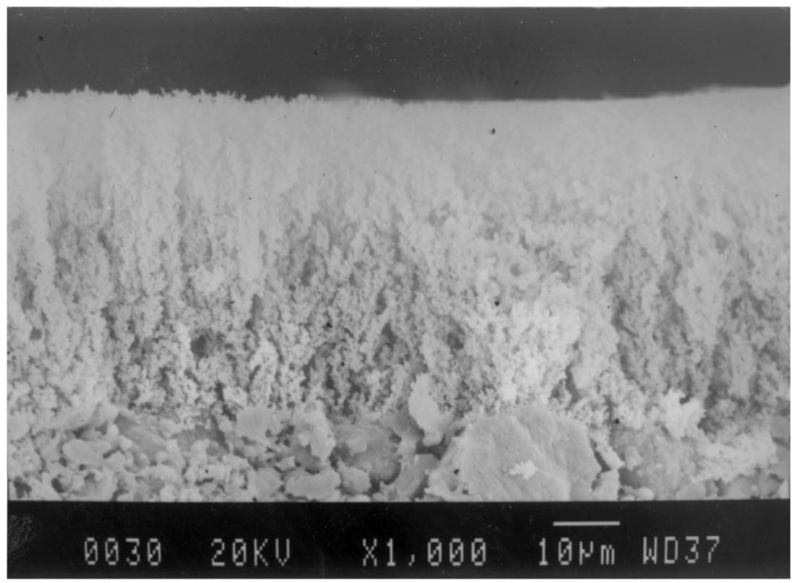

(c)

Figure 7 SEM pictures of (a) a plain porous ceramic substrate, (b) top-view, and (c) cross-sectional view of the ceramic substrate with TiO_2 deposits at the reactor entrance under the base condition.

450, and 550 °C, respectively. At these locations, the local temperatures (shall be termed the deposition temperature T_d from here on) as measured by a thermocouple are 330, 330, and 340 °C, respectively. This shows that thermal decomposition of TTIP and accompanying coagulation growth and deposition of TiO_2 can occur rapidly at ∼330 °C. Since with a higher T_f, the T_d reaches 330 °C at a location closer to the reactor entrance, the deposition flux peak shifts to the left, closer to the reactor entrance, with increasing T_f. Note also the deposition flux distribution becomes narrower but with a higher peak when T_f is raised. This is expected since the incoming rate of reactants and thus the total amount of TiO_2 produced are kept roughly constant, and the higher T_f results in more intense reaction, growth, and deposition around the peak area.

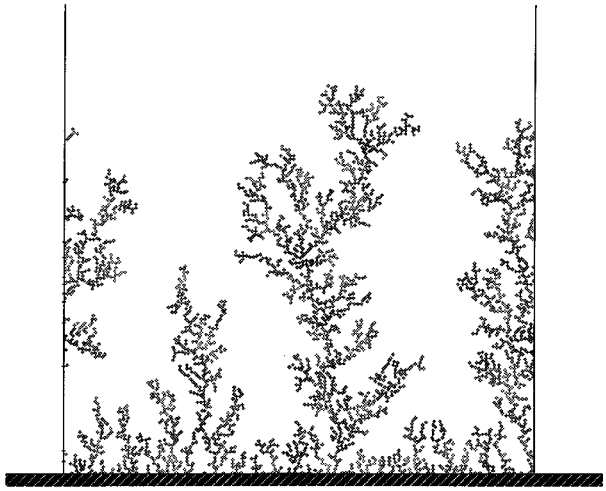

Figure 8 Cross-sectional view of a particle deposition structure obtained from a two-dimensional deposition simulation conducted by Tsai [14].

3.2. Formation mechanism, composition, phases, and sizes of TiO_2 deposits

In the present study, TiO_2 particles can be produced from TTIP through two different routes, one from thermal decomposition and the other from hydrolysis. The chemical equations for these two reactions are as follows:

$$\mathrm{Ti(O\text{-}\textit{i}\text{-}C_3H_7)_4} \rightarrow \mathrm{TiO_2 + 4C_3H_6 + 2H_2O}$$

for thermal decomposition

$$\mathrm{Ti(O\text{-}\textit{i}\text{-}C_3H_7)_4 + 2H_2O} \rightarrow \mathrm{TiO_2 + 4C_3H_7OH}$$

for hydrolysis

The reaction kinetics have been studied by Okuyama *et al.* [13] for the thermal decomposition reaction and by Kashima and Sugiyama [14] for the hydrolysis reaction.

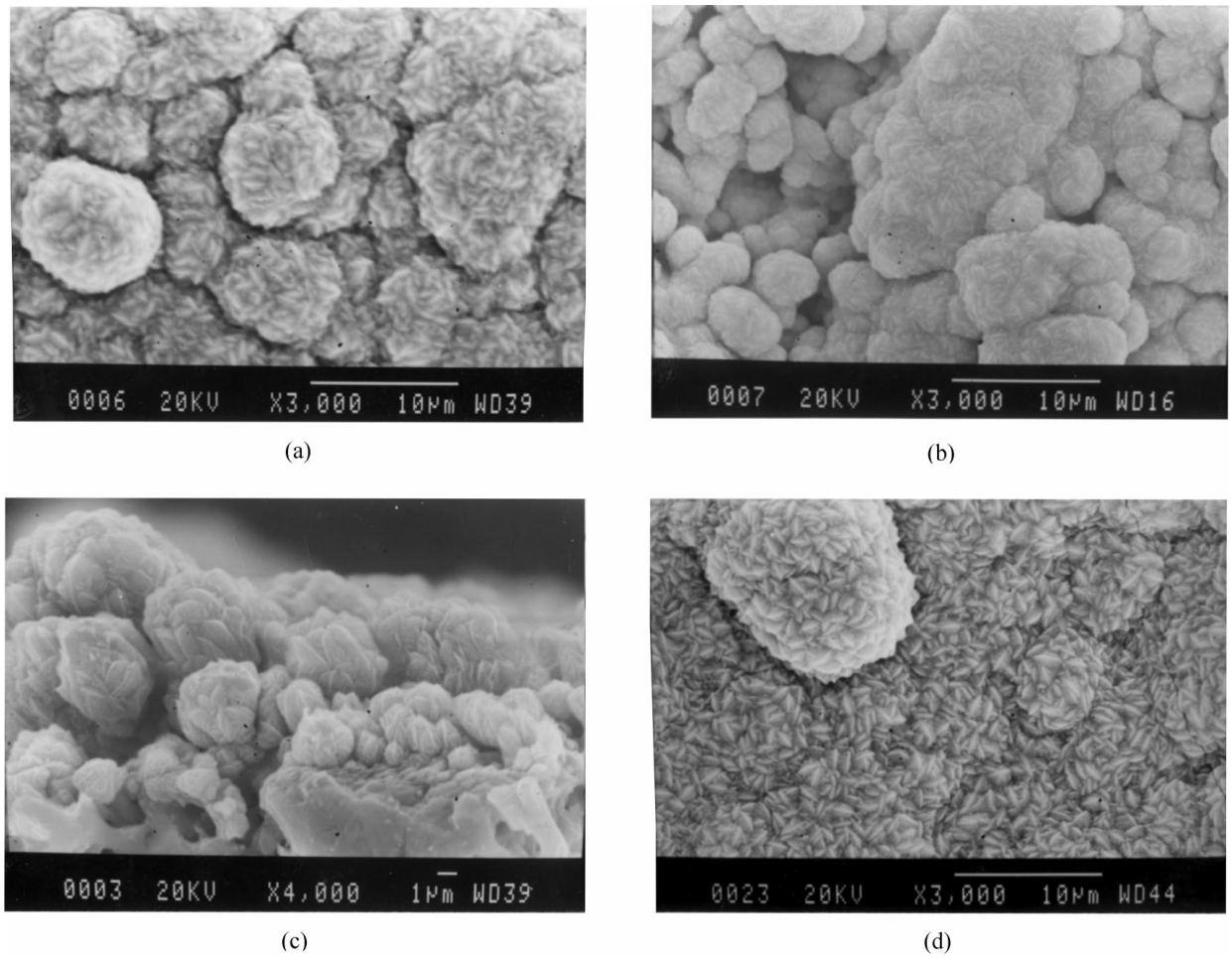

Figure 9 SEM pictures of TiO_2 deposits on the ceramic substrate with $C_{TTIP} = 3.6 \times 10^{-5}$ mol/l and $Q_t = 1{,}179$ sccm: (a) top-view for $T_f = 350$ °C and $x = 20$ cm ($T_d = 305$ °C), (b) top-view for $T_f = 450$ °C and $x = 12$ cm ($T_d = 303$ °C), (c) cross-sectional view for $T_f = 450$ °C and $x = 12$ cm ($T_d = 303$ °C), and (d) top-view for $T_f = 550$ °C and $x = 8$ cm ($T_d = 300$ °C).

They found that these two reactions are first order reactions with pre-exponential factors of 3.0×10^{15} and 3.96×10^{5} s^{-1} and activation energies of 8.43 and 70.5 kJ/g-mol for the hydrolysis and thermal decomposition reactions, respectively. From the values of the pre-exponential factor and activation energy, one readily sees that hydrolysis can occur much faster and easier than thermal decomposition. In our experimental procedure, water is excluded from the reaction system at the beginning. However, from the above two chemical equations, it is evident that water will be produced as a side product of the thermal decomposition reaction, and kicks off the hydrolysis reaction. This can be used to explain why there are TiO_2 deposits in regions before and near the reactor entrance, where T_d are less than 200 °C and not high enough to start the thermal decomposition. In fact, during the experiments, the deposit has been observed to grow from inside out at the reactor entrance region. We have also run the experiments at T_f of 100 and 200 °C, and cannot detect any deposit for the whole reactor. In conclusion, the deposit formed around the reactor entrance region is due to the hydrolysis invoked by water produced within the reactor from the thermal decomposition of TTIP.

Another interesting observation is that the deposit at the reactor entrance and exit regions is white while that within the rector is brown. To find out what makes the deposit brown, we have collected these brown deposits on a silicon substrate and run an ESCA on the deposit, and found some amount of carbon besides titanium and oxygen. Fig. 3 shows the ESCA result. The amount of

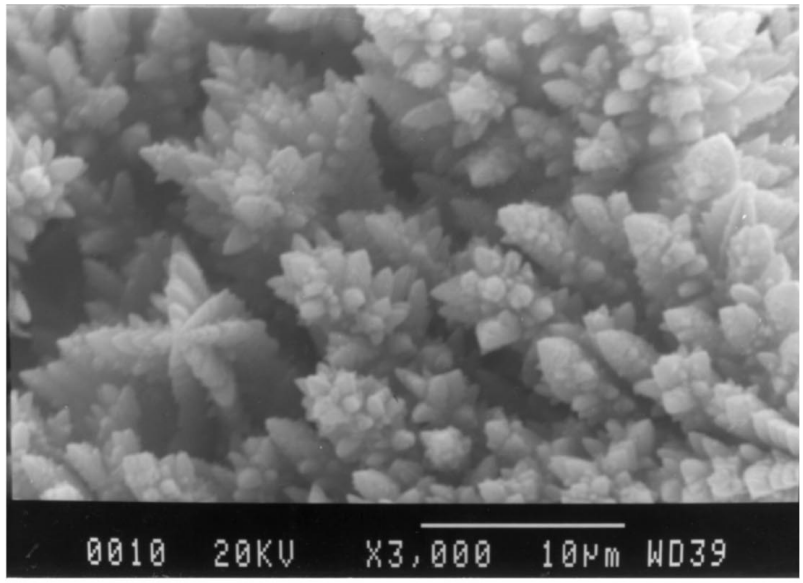

(a)

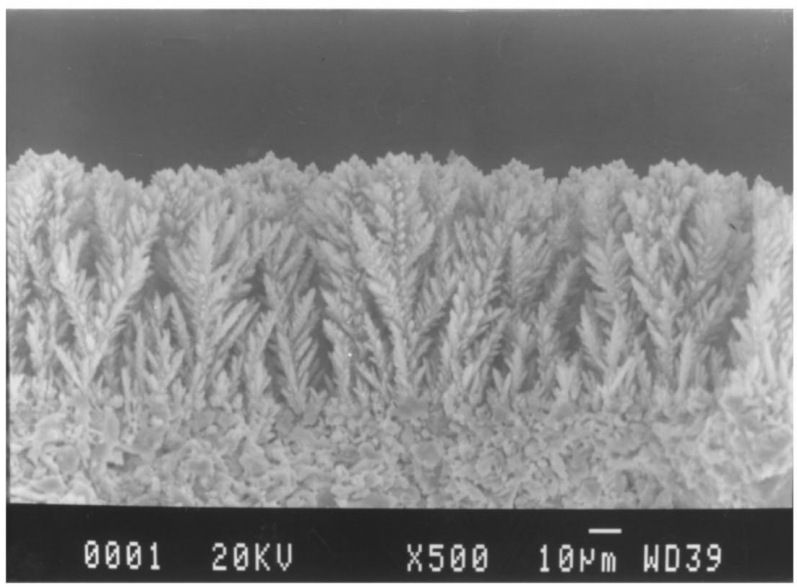

(b)

Figure 10 SEM pictures of TiO_2 deposits on the ceramic substrate with $T_f = 450$ °C, $C_{TTIP} = 3.6 \times 10^{-5}$ mol/l, and $Q_t = 1{,}179$ sccm at $x = 16$ cm ($T_d = 380$ °C): (a) top-view, (b) cross-sectional view.

carbon in the deposit is further found to be 9.2% by weight. We have also annealed in an air atmosphere the deposits collected by the quartz rings, and found a weight loss of 11–15% for the brown deposit while there is no appreciable weight loss for the white deposit formed at the reactor entrance and exit regions. This is because the carbon of the brown deposit is oxidized by oxygen to form CO_2 and escapes. If annealed in a 5×10^{-3} torr vacuum condition, there is no weight loss and the color of the deposit remains brown. The weight loss result is shown in Fig. 4. Note the annealing result is in reasonable agreement with the ESCA finding. Evidently, the carbon in the brown deposit comes from the further decomposition of the side products C_3H_6 and C_3H_7OH.

The powder X-ray diffraction on the deposit collected at $x = 0$ (reactor entrance), 15, and 67 cm (reactor exit) before and after annealing at 700 °C in an air atmosphere for three hours are shown in Fig. 5. By comparison with standard X-ray diffraction patterns of anatase and rutile phases of TiO_2, we found that before annealing particles at $x = 0$ cm are mostly amorphous while those at $x = 15$ and 67 cm are anatase phase. After annealing, the X-ray diffraction patterns at all three locations show strong anatase characteristics. No rutile phase is formed. Note that T_d of $x = 67$ cm is ~90 °C and yet particles collected there are anatase. This fact implies that these particles are formed in the early part of the reactor, but do not have the chance to deposit until the thermophoretic force kicks in at the reactor exit region.

The size distribution of these deposited TiO_2 particles is determined by the Otsuka Electronics LPA-300 particle size analyzer. This particle size analyzer uses two methods: light scattering for particles less than 1 μm and natural sedimentation for particles larger than 1 μm. From Fig. 6, it is clear that particles deposited within the reactor are bigger than those deposited at the

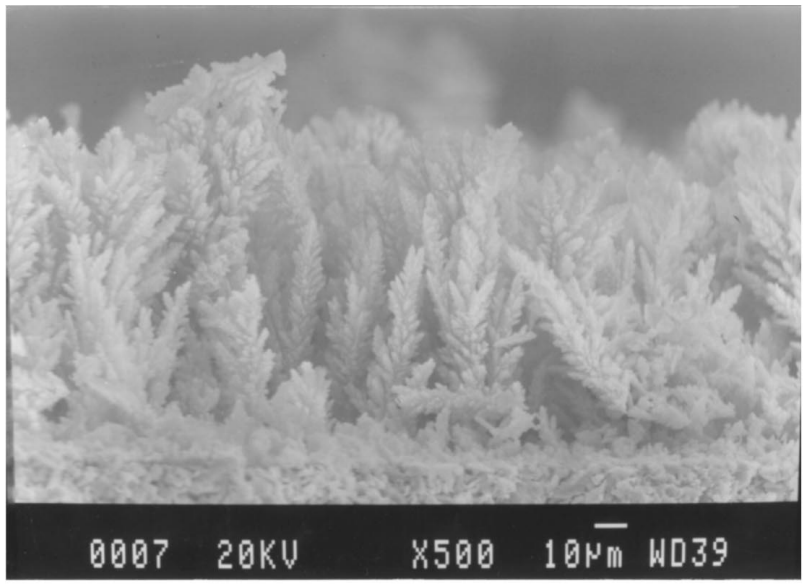

(a)

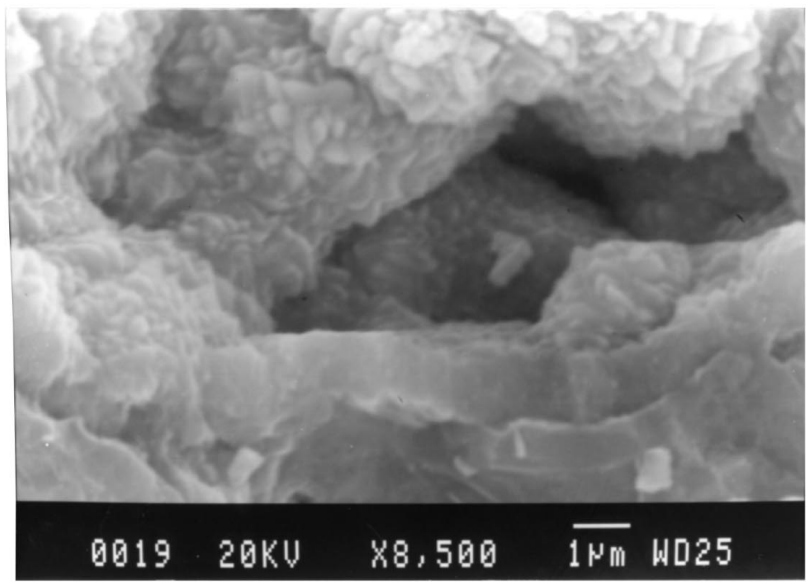

(b)

Figure 11 Cross-sectional SEM pictures of TiO_2 deposits on the ceramic disk with $C_{TTIP} = 3.6 \times 10^{-5}$ mol/l and $Q_t = 1{,}179$ sccm: (a) $T_f = 450$ °C, $x = 16$ cm, and $T_d = 380$ °C, (b) $T_f = 350$ °C, $x = 21$ cm, and $T_d = 310$ °C.

reactor entrance, which in turn are bigger than those deposited at the reactor exit.

3.3. Morphology of TiO_2 deposits

Fig. 7a shows the cross-sectional SEM of a plain ceramic substrate. It has a pore size of approximately 1–2 μm. The top-view and cross-sectional view of SEM pictures of TiO_2 deposited on ceramic substrates placed at the reactor entrance under the base condition are shown in Figs 7b and c, respectively. From the cross-sectional SEM picture, it can be seen that the whole structure is forest-like with each branch of the tree consisting of linearly packed spherical particles. This structure suggests that the particles are formed through a gas phase reaction in the main stream followed by coagulation growth, and deposit onto the substrate by diffusional transport. A simulation work done by Tsai [15] on particle deposition dominated by the diffusional transport in a two-dimensional domain shows a similar structure (Fig. 8). The morphology of TiO_2 deposits at the reactor exit is similar to that at the reactor entrance, only the packing spheres are smaller.

As to the deposit morphology within the reactor, it shows two very different structures. This structure difference has a strong correlation to the deposition

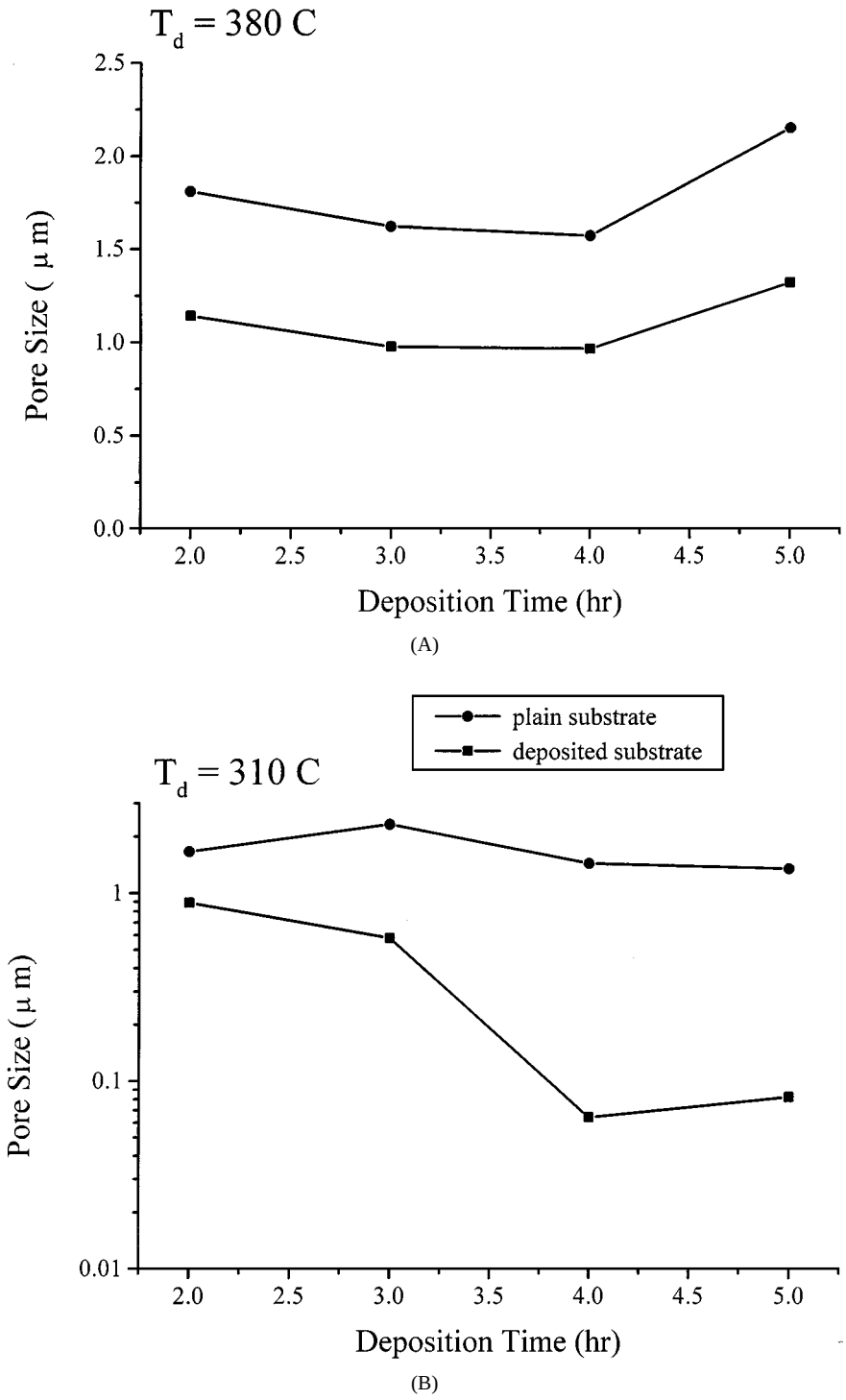

Figure 12 Pore sizes of ceramic disks before and after pore size reduction by TiO_2 deposits as a function of deposition time for condition (A) and condition (B).

temperature. In Fig. 9, SEM pictures obtained from T_f of 350, 450 and 550 °C, but at different locations ($x = 20$, 12, and 8 cm, respectively) are shown. At these locations under the corresponding T_f, the deposition temperatures are 305, 303, and 300 °C, respectively. Here, Figs 9a, b, and d are the top view for deposits resulting from T_f of 350, 450 and 550 °C, respectively, and Fig. 9c is the cross-sectional view for deposits from T_f of 450 °C. The particles are rock-like and the structure is a packing of rocks. The boundary between rocks becomes less distinguishable as T_f increases, possibly due to the increasing sintering extent and increasing deposition amount. These deposits possess a good adhesivity to the substrate as judged from the Scotch test.

The morphology of TiO_2 deposits within the reactor at a higher deposition temperature is shown in Fig. 10. Fig. 10a shows the top view while Fig. 10b the cross-sectional view for deposits from the base condition. The substrate is placed at $x = 16$ cm where the deposition temperature is 380 °C. The structure is also forest-like but with each tree being more of crystal form. These deposits appear to have a poor adhesivity to the substrate.

A theory can be proposed for the dramatic difference in deposit structure resulting from the difference in the deposition temperature. For a higher T_d, the particles are formed more from the bulk gas phase reaction and homogeneous nucleation. After the coagulation growth, the particles deposit onto the substrate due to diffusional transport. The forest-like structure is a characteristics of the diffusional deposition, and appears to have a weak attachment with the substrate. When the deposition temperature is lower, the gas phase reaction is less likely to occur than the surface reaction. Therefore, the particles are formed more from the surface reaction and heterogeneous nucleation. The result is a strong association with the substrate.

Except T_d, other operating conditions such as C_{TTIP} and Q_t are found not to affect the deposit morphology in a significant extent, neither does the annealing at 700 °C in an air atmosphere for three hours. The annealing only makes the deposit more rounded because of the sintering.

3.4. Surface modification of ceramic disks

The ceramic disks are placed, perpendicular to the gas flow, between two quartz rings to prevent it from falling down. A stainless rod is also placed behind the quartz ring to prevent the ceramic disk from sliding during the evacuation process. Two experimental conditions are chosen: (A) $T_f = 450$ °C and $x = 16$ cm ($T_d = 380$ °C); (B) $T_f = 350$ °C and $x = 21$ cm ($T_d = 310$ °C). Particles collected under condition (A) are again in a forest-like structure while those collected under condition (B) are like rough rocks as shown in Fig. 11. Here, Fig. 11a is the cross-sectional view for deposits from condition (A) and Fig. 11b is the cross-sectional view for the interior of the substrate deposited under condition (B). It is clear from Fig. 11b that the deposit forms even in the interior of the substrate. This observation supports our theory that at lower deposition temperatures the surface reaction route is more dominant, because otherwise it will be difficult for the particles formed in the bulk to penetrate the substrate and deposit onto the interior of the substrate.

The pore size reduction achieved by the deposition under conditions (A) and (B) can be determined by the N_2 gas permeation experiments conducted before and after the deposition. Fig. 12 shows the pore size of the substrate before and after the deposition as a function of deposition time. It is evident from the figure that under condition (A) the pore size reduction achieved is very limited while that for the condition (B) is quite dramatic if a sufficiently long deposition time is used. The pore size reduction effect of condition (B) seems to reach a limit after 4 h of deposition while that of the condition (A) appears to be invariant with respect to the deposition time. Note the plain ceramic disk used possesses a pore size of approximately 1–2 μm and thus the pore size of the plain substrate varies slightly from one data point to the other as shown in Fig. 12.

4. Conclusions

The morphology and pore size reduction effectiveness of TiO_2 deposits, produced through a CVD process using TTIP as the precursor, were investigated. The experimental data showed that the deposit characteristics is a strong function of the deposition temperature and is invariant with respect to the flow rate and concentration of the reactant stream. At a deposition temperature of about 300 °C, we were able to reduce the pore size of a porous ceramic substrate from about 1–2 μm down to about 64 nm with a deposition time of 4 h and the resulting TiO_2 layer, which is a packing rock structure, has a good adhesivity to the substrate. On the other hand, if the deposition temperature was raised to about 380 °C, the resulting TiO_2 deposit was a forest-like structure, had a poor adhesivity to the substrate, and produced only minor reduction in pore size of the substrate.

Acknowledgement

The authors would like to thank Mr. Tsing-Ming Tsai, Mr. Chung-Tai Huang, and Mr. Jyh-Ching Tsai of our department for their assistance in theoretical modeling, synthesis of ceramic substrates, and carrying out BET experiments, respectively. We are also indebted to the support of the National Science Council of the Republic of China under grant NSC 86-2214-E-007-007 and National Tsing-Hua University for the postdoctoral researcher fund (Dr. Shu-Chuan Huang).

References

1. J. H. BRAUN, A. BAIDINS and R. E. MARGANSKI, *Prog. Organic Coatings* **20** (1992) 105.
2. G. P. FOTOU, S. VEMURY and S. E. PRATSINIS, *Chem. Eng. Sci.* **49** (1994) 4934.
3. R. HUTTER, D. C. M. DUTOIT, T. MALLAT, M. SCHNEIDER and A. BAIKER, *J. Chem. Soc. Chem. Commun.* (2) (1995) 163.
4. G. D. ULRICH, *Chem. & Eng. News* **62** (1984) 22.
5. S. E. PRATSINIS, *Chem. Eng. Prog.* **85** (1989) 62.
6. M. TSAPATSIS and G. R. GAVALAS, *AIChE J.* **38** (1992) 847.

7. G. XOMERITAKIS and Y.-S. LIN, *Chem. Eng. Sci.* **49** (1994) 3909.
8. S. YAN, H. MAEDA, K. KUSAKABE, S. MOROOKA and Y. AKIYAMA, *Ind. Eng. Chem. Res.* **33** (1994) 2096.
9. K. S. CHOU, C. Y. CHEN and C. T. HUANG, *J. Chin. Inst. Chem. Engrs.* **29** (1998) 1.
10. P. UCHYLTIL, Z. WAGNER, J. ROCEK and Z. BROZ, *J. Membrane Sci.* **103** (1995) 151.
11. F. KIRKBIR and H. KOMIYAMA, *Canad. J. Chem. Eng.* **65** (1987) 759.
12. S.-Y. LU, H.-C. LIN and C.-H. LIN, *J. Crystal Growth* **200** (1999) 527.
13. K. OKUYAMA, R. USHIO, Y. KOUSAKA, R. C. FLAGAN and J. H. SEINFELD, *AIChE J.* **36** (1990) 409.
14. K. KASHIMA and H. SUGIYAMA, *Kagaku Kogaku Ronbunsyu* **16** (1990) 551.
15. C.-M. TSAI, "Particle Deposition, Resulting Microstructure, and Effective Transport Properties in such Microstructure within Chemical Vapor Deposition Reactors," MS thesis (in Chinese), National Tsing-Hua University, Taiwan, Republic of China, 1997.

Received 14 October 1997
and accepted 2 March 1999